PHYSICAL REVIEW A **83**, 041403(R) (2011)

Nonadiabatic molecular high-order harmonic generation from polar molecules: Spectral redshift

Xue-Bin Bian and André D. Bandrauk*

Département de Chimie, Université de Sherbrooke, Sherbrooke, Quebéc, Canada J1K 2R1

(Received 8 February 2011; published 22 April 2011)

Molecular high-order harmonic generation (MHOHG) from the polar diatomic molecule HeH^{2+} in short intense laser fields is studied numerically. Due to the nonadiabatic response of the molecular dipole to the rapid change of laser intensity, a spectral redshift is predicted in high-intensity and ultrashort laser pulses, contrary to the blueshift observed in the harmonics generated from atoms in long laser pulses. The MHOHG temporal structures are investigated by a wavelet time-frequency analysis, which shows that the enhanced excitation of localized long lifetime excited states shifts the harmonic generation spectrum in the falling part of short laser pulses, due to the presence of a permanent dipole moment, and thus is unique to polar molecules.

DOI: 10.1103/PhysRevA.83.041403 PACS number(s): 33.80.Rv, 42.65.Ky, 34.50.Gb

High-order harmonic generation (HHG) has become an important tool to generate coherent attosecond (1 as $= 10^{-18}$ s) laser pulses [1]. It provides us with an important coherent optical source to investigate ultrafast electronic dynamics [2–5]. Usually, HHG comes from the interaction between intense laser pulses and atoms [2,4], molecules [5], and plasmas [6]. The general feature of HHG spectra is a rapid decay of the lower-order harmonics, then a long plateau, and a short cutoff with photon energy around $I_p + 3.17U_p$ (where I_p is the ionization potential and $U_p = I/4\omega^2$ denotes the ponderomotive energy). Currently, a semiclassical three-step model is used to interpret the HHG mechanism for initial zero velocity ionized electrons [7] and nonzero velocity electrons [8]. In this model, when atoms and molecules are exposed to intense laser fields, the electron can be ionized by tunneling from the ground state. It is then accelerated by the laser field, and returns back to the original ion to recombine with the parent ion and emit HHG photons due to a phase change of the electric field. This model is successful in explaining the maximum cutoff energy $I_p + 3.17U_p$ of HHG observed in atoms and molecules [5]. However, cutoff energies larger than $I_p + 3.17U_p$ can be obtained in a laser-induced electron transfer (LIET) with the neighboring ions [9–12] in molecules and is called molecular high-order harmonic generation (MHOHG).

Recent progress in ultrafast optics has allowed the generation of ultraintense laser pulses comprising only a few field oscillation cycles [2]. The change of amplitude of the electric field during one optical cycle is not negligible. One of the central questions concerns this *nonadiabatic* response effect [13] of atoms and molecules to the short high-intensity laser fields. The temporal and spectral structures of HHG from atoms have been well studied previously [14–19]. Most of the theoretical [14,15] and experimental [16–18] results show spectral blueshift for atoms in intense laser pulses. The spectral blueshift mainly comes from two physical processes. One is predicted by the strong-field approximation (SFA) model [20,21]. The electron ionized on the rising part of the laser field will experience additional accelerations and acquire more energy, which will lead to a blueshift in the HHG spectra [22]. The other process is one in which the ionized electron changes the refractive index of the ionized media [23]. This propagation effect leads to an additional blueshift in HHG [17–19]. A spectral redshift is observed in laser cluster interaction [24] and harmonics from the multiphoton ionization of atoms interacting with a long laser-pulse field (300 ps) [25]. However, this reported redshift is also explained by the propagation effect because of the change of the index of refraction. To our knowledge, except for the propagation effect, no redshift has been reported in either atomic or molecular HHG. In this Rapid Communication, we will show the spectral redshift in the MHOHG from polar molecules with short intense laser pulses.

Due to the permanent dipole, polar molecules have received increasing attention recently [26–28]. The phenomena of enhanced excitation (EE) and enhanced ionization (EI) have been reported [26]. The Stark shift of the ionization potential leads to a higher cutoff energy of MHOHG [27]. The long lifetime of excited states leads to strong resonance and multichannel MHOHG in the harmonic spectrum [12]. In this Rapid Communication, we probe the nonadiabatic effects [29] in the temporal and spectral structures of MHOHG from the model asymmetric diatomic molecule HeH^{2+} in short intense laser pulses. The MHOHG spectra of HeH^{2+} are obtained by numerically solving the time-dependent Schrödinger equation (TDSE). For computational details, we refer to Refs. [30,31] for this one-electron system. The internuclear distance R is fixed at 4 a.u. (near the excited-state minimum $R = 3.89$ a.u.). The energies of the ground state $1s\sigma$ and the first excited state $2p\sigma$ are -2.25 and -1.03 a.u., respectively. The initial state for time evolution is the ground state $1s\sigma$. The laser polarization is along the molecular axis. The electric field of the laser pulse is given by $E(t) = E_0 f(t)\cos(\omega t)$, $t \in [-\tau/2, \tau/2]$, with the pulse shape $f(t) = \cos^2(\pi t/\tau)$, where τ is the total duration of the laser pulses. Thus the total electric-field area is zero. The power spectra of MHOHG is calculated by Fourier transformation of the dipole momentum in acceleration form $d_A(t)$, as it is the most reliable numerical method for strong-field interactions [32], thus avoiding transient effects in very short pulses.

A MHOHG spectrum of HeH^{2+} in laser field at wavelength 400 nm and intensity $I = 3.3 \times 10^{15}\mathrm{W/cm^2}$ with a 15 cycle duration is shown in Fig. 1. A typical difference from the

*Andre.Bandrauk@USherbrooke.ca

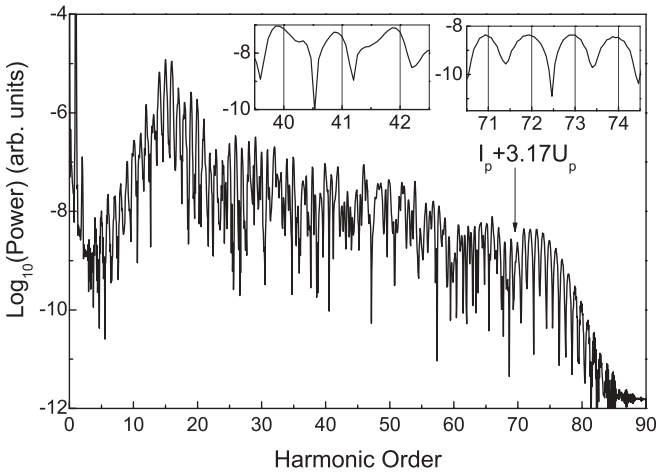

FIG. 1. (Color online) Spectrum of harmonics produced by HeH^{2+} exposed to a laser pulse at wavelength 400 nm. The pulse has a $\cos^2$ shape with a duration of 15 optical cycles. The peak laser intensity is $I = 3.3 \times 10^{15}$ W/cm^2. Inset: spectral structure of some harmonics illustrating the presence of redshifted even and odd harmonics.

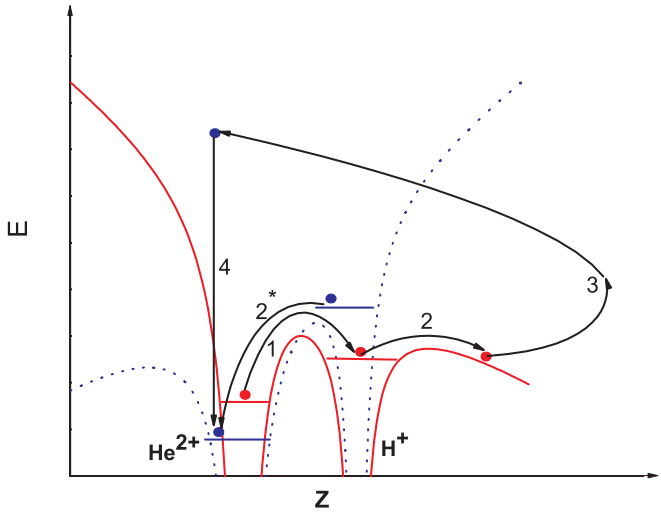

FIG. 2. (Color online) Schematic illustration of the four-step model of MHOHG in HeH^{2+}. Step (1): The laser field pumps the electron from the ground state to the localized long lifetime excited state; part of the electron is ionized from the excited state in step (2), then accelerated in the laser field in step (3), and then transits back to the ground state to emit photons in step (4). Part of the electron on the excited state will directly transit to the ground state in step (2*) when the laser field changes its direction (phase). This leads to a strong resonance in the harmonic spectra. The Stark shift of the energy levels is included.

usual HHG spectra of neural atoms and molecules is the strong resonance around harmonic order 15. The harmonic conversion efficiency is about three orders higher than the harmonics in the long plateau, which can be used to generate bright attosecond pulses (trains). The strong resonance in MHOHG cannot be explained consistently by the three-step model [7]. The cutoff energy in MHOHG in Fig. 1 is larger than the maximum $I_p + 3.17U_p$ obtained by the three-step model [7,8]. The semiclassical three-step model mainly takes the ground and continuum states into account. It is valid for neutral atoms and symmetric molecules, since the lifetime of the corresponding excited states is comparably short in intense laser fields. However, for the asymmetric molecular ions, such as HeH^{2+}, LiH^{3+}, and BeH^{4+}, which have permanent dipoles and multiple centers, the lifetime of the corresponding excited states may be comparably as long as the pulse. For example, the first excited $2p\sigma$ state of HeH^{2+} is a localized state on the H atom, and the mean lifetime is about 4 ns [33]. In this case, there can be considerable population created on the ground and low excited states in intense laser pulses. Clearly, the role of excited states must be considered as it may provide us with new mechanisms for attosecond science. Next, we will show that a four-step model [12,34,35] is more appropriate to interpret the resonance and the larger cutoff energy.

The four-step model in the resonant polar system is illustrated in Fig. 2, i.e., preexcitation to a localized long lifetime resonant state, tunneling ionization from the resonance state, acceleration in the laser field, and recombination to the ground state. In particular, part of the electrons populated on the $2p\sigma$ state by EE may transit back to the ground state directly when the laser field changes its direction (phase), which will lead to a strong resonance in the MHOHG spectra. The resonant position around the harmonic order 15 in the MHOHG spectrum agrees well with the calculated dressed energy difference between the first excited state and the ground state [12]. The larger cutoff energy comes from the additional acceleration for an electron recombining with the neighboring ion. This mechanism has been confirmed by classical simulations [12]. The cutoff energy and the recombination time agree well with the quantum results. To further identify the role of excited states, we perform a time profile analysis of the harmonic spectra to probe the temporal structures. The time profile of harmonic ω_q is obtained by a wavelet analysis [36,37]: $d(\omega_q,t) = \int d_A(t) w_{t,\omega_q}(t')dt'$, with the wavelet kernel $w_{t,\omega_q}(t') = \sqrt{\omega_q} W[\omega_q(t'-t)]$. The mother wavelet we use is a Morlet wavelet: $W(x) = (1/\sqrt{\sigma})e^{ix}e^{-x^2/2\sigma^2}$. In this Rapid

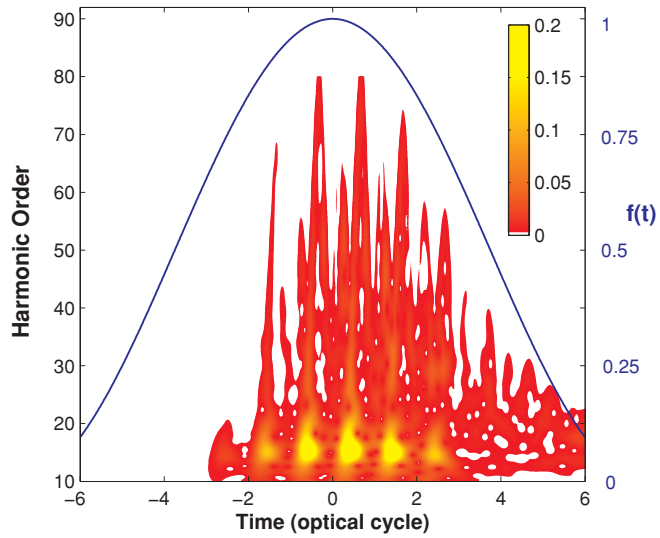

FIG. 3. (Color online) Wavelet analysis of the harmonic generation by HeH^{2+} and the pulse-shape function $f(t)$ of the intense laser field. The laser parameters are the same as those in Fig. 1.

Communication, we use $\sigma = 15$ a.u. The time profile of harmonic in Fig. 1 is presented in Fig. 3. From the figure, one can see an obvious resonance area around harmonic order 15. From the color bar, the amplitude of the signal around harmonic order 15 is one order higher than that of the harmonics in the plateau ($N = 30$–60). Evidence of the strong resonance of the first excited state in the time domain is strong support of the four-step model, which will help us understand the novel spectral structure of the harmonics.

Another important feature of the MHOHG spectra shown in the inset of Fig. 1 is the redshift of spectra. The redshift in the plateau is somewhat larger than the frequency shift around the cutoff. For the polar molecular HeH^{2+}, the Stark-shifted ionization potential $I_p(t)$ is time dependent. As previously pointed out by Kamta and Bandrauk [26], $I_p(t) \approx I_0 + RE(t)/2$, with I_0 the field-free ionization potential. From the SFA model [20], the accumulated phase of a free electron in a laser field is $S = \int_{t_i}^{t_f} [\frac{p^2}{2} + I_p(t)]dt$, where t_i is the time of ionization and t_f is the time of recollision. On the rising part of the laser pulse, $\frac{dS}{dI} > 0$, leading to spectral blueshift, while it leads to redshift on the falling part of the laser pulse. For atoms and neutral molecules in an intense laser field with an intensity lower than the saturation intensity I_s, the spectral shift on the rising part will cancel with the shift on the falling part, and no obvious shift appears in the HHG spectra. For laser intensities above the saturation intensity I_s, the blueshift is observed in atomic HHG experimentally. From the studies of atoms, when the laser intensity is beyond the saturation intensity I_s, the ionization mainly occurs on the rising part of the laser field, and the harmonics are generated on the rising part of the laser pulse. Compared to the constant laser amplitude, the rising laser intensity will lead to a longer acceleration of the electron and the extra energy will lead to the blueshift on the HHG spectra. Since the ionization potential of atoms is comparably small, electrons will be sufficiently ionized before the peak laser intensity for $I > I_s$. As a result, it is very difficult to control the harmonics generated on the falling part of the laser field. This is the main reason why the redshift is not produced in HHG from atoms. Although the redshift is observed by some experiments [24,25], it is due to the propagation effect of harmonics in a high refractive index medium induced by the ionized electron, and is not directly generated in the HHG process itself. As analyzed above, this redshift comes from the falling part of the laser field, which agrees well with our time profile results in Fig. 3. For lower-order harmonics, as shown in Fig. 3, the time profile mainly concentrates on the falling part of the pulse, which causes a larger redshift in the MHOHG spectra. However, from the semiclassical model, the harmonics near the cutoff mainly occur only around the peak laser intensity, which will be less influenced by the duration of the laser pulse. Since the change of laser intensity dI/dt is small near the peak, the temporal and spectral shifts near the cutoff are predicted to be small. This prediction agrees well with our results in Figs. 1 and 3.

Next, we explain why the redshifted harmonics are generated in the falling part of the laser pulse. We present the population of the $2p\sigma$ state and the total ionization rate $\Gamma(t)$ as a function of time in Fig. 4. $\Gamma(t)$ is obtained by the depletion rate of the population on the bound states: $\Gamma(t) = -\frac{dP(t)}{dt}$, where $P(t) = \sum_n |\langle\phi_n|\psi(t)\rangle|^2$ is the sum of probability on all

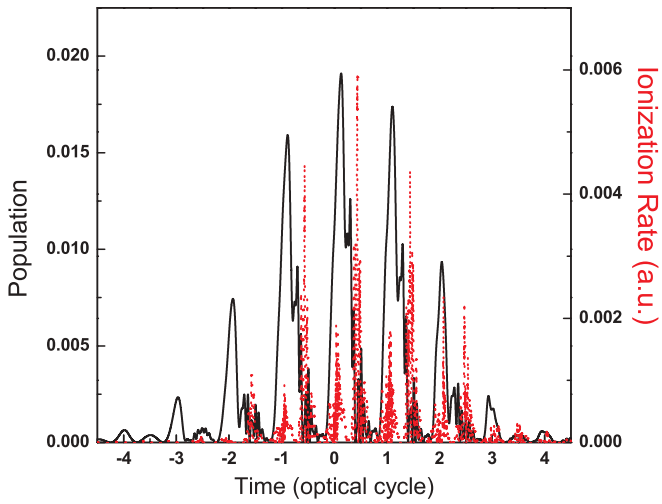

FIG. 4. (Color online) Population of the first excited state $2p\sigma$ (solid black line) and the total ionization rate (dotted red line) as a function of time. The laser parameters are the same as those in Fig. 1.

bound states $|\phi_n\rangle$. An obvious feature in Fig. 4 is that EE and EI are not *synchronous*. The intense laser field causes a small ionization directly from the ground state, and at the same time pumps the system to the first excited state. Due to the lower ionization potential I_p, the ionization rate of the excited states may be one order higher than the ground state [12,30], which leads to larger enhanced ionization from the excited states. From the above four-step model, the EI will have a time delay with respect to EE. Consequently, the EE of the long lifetime excited states plays a double role: suppressing the direct ionization from the ground state, and time shifting the EI in the falling part of the short laser field.

In fact, this nonadiabatic effect will be less noticeable for long laser pulses. We have calculated the HHG from HeH^{2+} in the laser field with the same wavelength and intensity as above, but with a different duration of laser pulses. We

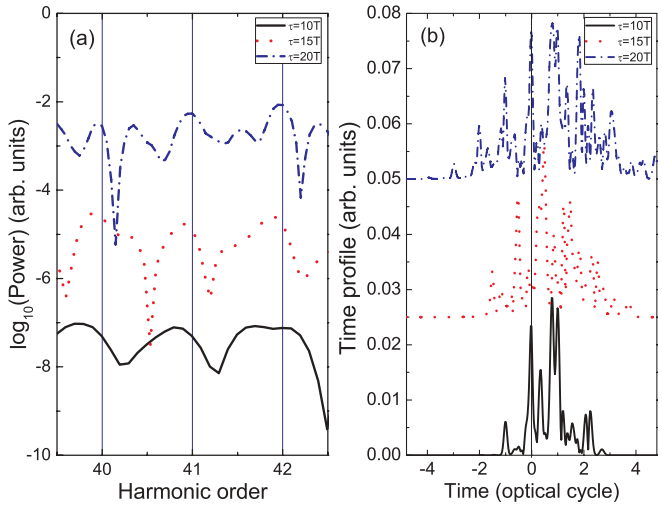

FIG. 5. (Color online) Redshifted harmonics N =40–42 (a) and the time profile of order $N = 40$ (b) at laser pulse durations 10, 15, and 20 optical cycles, respectively. The laser intensity and wavelength are the same as in Fig. 1.

take the harmonic order $N = 40$ as an example. When we increase the laser-pulse duration from 10 to 20 optical cycles, as shown in Fig. 5(a), the nonadiabatic spectral redshift gradually decreases. We plotted the corresponding time profile of harmonic $N = 40$ in Fig. 5(b). When the pulse duration increases, the nonadiabatic effect will be weaker and weaker, and the harmonic generation is gradually shifted from the falling part of the pulse to the rising part. The intensity-induced $dS/dI > 0$ on the rising part of the pulse will cancel with the $dS/dI < 0$ on the falling part of the pulse, which decreases the spectral redshift. Another feature for a long laser pulse (e.g., $\tau = 20T$ as shown in Fig. 5) is the resolution of multichannel MHOHG from the ground and excited states [12]. As the laser pulse becomes longer, the width of the harmonic spectra will be narrower, and a multiple frequency harmonic series from excited states will appear [12].

We next discuss the experimental access to observe the nonadiabatic redshift. HeH^{2+} is exotic for HHG experiments. However, we can use other polar molecules, such as HCl, CO, etc., because the mechanism is the same. Due to the change of the refractive index, the reported blueshift and redshift of harmonics are produced in short [16–18] (femtosecond time scale) and long [24,25] (picosecond time scale) laser fields, respectively. As a result, there will be no entanglement between the macroscopic redshift-propagation effect and the nonadiabatic redshift dynamics in short few-cycle laser pulses. To reduce the influence of the macroscopic blueshift-propagation effect in short pulses, we have to reduce the collective effect. We notice that the thin gas jet can be used to reflect the single-molecule response [38]. So, the experimental observation of nonadiabatic redshift is accessible.

In conclusion, we have explored the temporal and spectral structure of MHOHG from a resonant one-electron asymmetric molecular ion system HeH^{2+}. Due to the long lifetime of the resonant state, the EE of the resonance state leads to a delay of EI in short pulses, which makes the harmonic spectra redshifted in short laser pulses. Since the change of the laser intensity at the center of the pulse is quite small, the frequency shift in the cutoff region is smaller than the shift in the plateau. This spectral redshift is predicted independent of propagation effects. The importance of resonances of autoionizing states in HHG in plasma plumes [35,39] was reported recently. We predict that the redshift of HHG can also be observed experimentally by exposing plasmas to short intense laser pulses.

We thank Dr. K. J. Yuan and S. Chelkowski for helpful discussions. We also thank RQCHP and Compute Canada for access to massively parallel computer clusters.

[1] P. B. Corkum and F. Krausz, Nature Phys. **3**, 381 (2007).
[2] T. Brabec and F. Krausz, Rev. Mod. Phys. **72**, 545 (2000).
[3] H. Niikura, D. M. Villeneuve, and P. B. Corkum, Phys. Rev. Lett. **94**, 083003 (2005).
[4] M. V. Frolov *et al.*, Phys. Rev. Lett. **102**, 243901 (2009).
[5] A. D. Bandrauk, S. Barmaki, S. Chelkowski, and G. Lagmago Kamta, in *Progress in Ultrafast Intense Laser Science*, edited by K. Yamanouchi (Springer, New York, 2007), Vol. III.
[6] S. Kubodera *et al.*, Phys. Rev. A **48**, 4576 (1993).
[7] P. B. Corkum, Phys. Rev. Lett. **71**, 1994 (1993).
[8] A. D. Bandrauk, S. Chelkowski, and S. Goudreau, J. Mod. Opt. **52**, 411 (2005).
[9] A. D. Bandrauk, S. Barmaki, and G. L. Kamta, Phys. Rev. Lett. **98**, 013001 (2007).
[10] A. D. Bandrauk, S. Chelkowski, H. Yu, and E. Constant, Phys. Rev. A **56**, R2537 (1997).
[11] P. Moreno, L. Plaja, and L. Roso, Phys. Rev. A **55**, R1593 (1997).
[12] X. B. Bian and A. D. Bandrauk, Phys. Rev. Lett. **105**, 093903 (2010).
[13] M. Geissler, G. Tempea, and T. Brabec, Phys. Rev. A **62**, 033817 (2000).
[14] C. Kan, C. E. Capjack, R. Rankin, and N. H. Burnett, Phys. Rev. A **52**, R4336 (1995).
[15] J. B. Watson, A. Sanpera, and K. Burnett, Phys. Rev. A **51**, 1458 (1995).
[16] H. J. Shin, D. G. Lee, Y. H. Cha, K. H. Hong, and C. H. Nam, Phys. Rev. Lett. **83**, 2544 (1999).
[17] C.-G. Wahlström *et al.*, Phys. Rev. A **48**, 4709 (1993).
[18] K. Miyazaki and H. Takada, Phys. Rev. A **52**, 3007 (1995).
[19] J. J. Macklin, J. D. Kmetec, and C. L. Gordon III, Phys. Rev. Lett. **70**, 766 (1993).
[20] M. Lewenstein, P. Balcou, M. Y. Ivanov, A. L'Huillier, and P. B. Corkum, Phys. Rev. A **49**, 2117 (1994).
[21] P. Salières *et al.*, Science **292**, 902 (2001).
[22] K. J. Schafer and K. C. Kulander, Phys. Rev. Lett. **78**, 638 (1997).
[23] W. M. Wood, C. W. Siders, and M. C. Downer, Phys. Rev. Lett. **67**, 3523 (1991).
[24] K. Y. Kim *et al.*, Phys. Rev. A **71**, 011201(R) (2005).
[25] F. Brandi, F. Giammanco, and W. Ubachs, Phys. Rev. Lett. **96**, 123904 (2006).
[26] G. L. Kamta and A. D. Bandrauk, Phys. Rev. Lett. **94**, 203003 (2005).
[27] A. Etches and L. B. Madsen, J. Phys. B **43**, 155602 (2010).
[28] H. Akagi *et al.*, Science **325**, 1364 (2009).
[29] I. P. Christov *et al.*, Phys. Rev. Lett. **77**, 1743 (1996).
[30] X. B. Bian and A. D. Bandrauk, Phys. Rev. A **83**, 023414 (2011).
[31] X. B. Bian, L. Y. Peng, and T. Y. Shi, Phys. Rev. A **77**, 063415 (2008); **78**, 053408 (2008).
[32] A. D. Bandrauk, S. Chelkowski, D. J. Diestler, J. Manz, and K. J. Yuan, Phys. Rev. A **79**, 023403 (2009).
[33] I. Ben-Itzhak, I. Gertner, C. Heber, and B. Rosner, Phys. Rev. Lett. **71**, 1347 (1993).
[34] D. B. Milošević, Phys. Rev. A **81**, 023802 (2010).
[35] V. Strelkov, Phys. Rev. Lett. **104**, 123901 (2010).
[36] P. Antoine, B. Piraux, and A. Maquet, Phys. Rev. A **51**, R1750 (1995).
[37] C. Chandre, S. Wiggins, and T. Uzer, Physica D **181**, 171 (2003).
[38] A. D. Shiner *et al.*, Phys. Rev. Lett. **103**, 073902 (2009).
[39] R. A. Ganeev *et al.*, Opt. Lett. **31**, 1699 (2006).